*Natural Resources Research (© 2021)*
https://doi.org/10.1007/s11053-021-09896-4

*Original Paper*

# Predicting Blast-Induced Ground Vibration in Open-Pit Mines Using Different Nature-Inspired Optimization Algorithms and Deep Neural Network

**Hoang Nguyen,[1,4] Xuan-Nam Bui,[1,2] Quang-Hieu Tran,[1,2] Dinh-An Nguyen,[1] Le Thi Thu Hoa,[1] Qui-Thao Le,[1,2] and Le Thi Huong Giang[3]**

*Received 29 January 2021; accepted 30 May 2021*

Blast-induced ground vibration (GV) is a hazardous phenomenon in open-pit mines, and it has unquestionable effects, such as slope instability, deformation of structures, and changing the flow direction of groundwater. Therefore, many studies in recent years have focused on the accurate prediction and control of GV in open-pit mines. In this study, three intelligent hybrid models were examined for predicting GV based on different nature-inspired optimization algorithms and deep neural networks. Accordingly, a deep neural network (DNN) was developed for predicting GV under the enhancement of deep learning techniques. Subsequently, aiming at improving the accuracy and reducing the error of the DNN model in terms of the prediction of blast-induced GVs, three optimization algorithms based on the behaviors of whale, Harris hawks, and particle swarm in nature (abbreviated as WOA, HHOA, and PSOA, respectively) were considered and applied, namely HHOA–DNN, WOA–DNN, and PSOA–DNN, respectively. The results were then compared with those of the conventional DNN model through various performance indices; 229 blasting events in an open-pit coal mine in Vietnam were processed for this aim. Finally, it was found that the proposed intelligent hybrid models outperform the DNN model with deep learning techniques, although it is a state-of-the-art model that has been recommended and claimed by previous researchers. In particular, HHOA, WOA, and PSOA (with global optimization) further improved the accuracy of the DNN model by 1–2%. Of those, the HHOA–DNN model provided the highest performance with a mean-squared-error of 2.361, root mean squared error of 1.537, mean absolute percentage error of 0.123, variance accounted for of 93.015, and coefficient determination of 0.930 on the testing dataset. The findings also revealed that the explosive charge per blast, monitoring distance, and time delay per each blasting group are necessary parameters for predicting GV.

**KEY WORDS:** Mine blasting, Peak particle velocity, Ground vibration, Nature-based optimization algorithm, Deep neural network, Harris hawks optimization.

[1]Department of Surface Mining, Mining Faculty, Hanoi University of Mining and Geology, 18 Vien Str., Duc Thang Ward, Bac Tu Liem Dist., Hanoi 100000, Vietnam.
[2]Innovations for Sustainable and Responsible Mining (ISRM) Group, Hanoi University of Mining and Geology, 18 Vien Str., Duc Thang Ward, Bac Tu Liem Dist., Hanoi 100000, Vietnam.
[3]Mathematics Department, Faculty of Sciences, Hanoi University of Mining and Geology, 18 Vien Str., Duc Thang Ward, Bac Tu Liem Dist., Hanoi 100000, Vietnam.
[4]To whom correspondence should be addressed; e-mail: nguyenhoang@humg.edu.vn

## INTRODUCTION

In open-pit mines (OPMs), the drilling-blasting method is used as a highly effective technique for breaking and removing rock mass. Once drilling machines create boreholes, explosive materials are



Published online: 12 July 2021

(a)

(b)

**Figure 1.** Significant effects induced by GVs of blasting operations in OPMs: **a** cracking of structures; **b** slope failure.

charged into them and then detonated (Guo et al., 2019; Nguyen et al., 2020; Zhang et al., 2020a, 2020b). The explosive energy (EE) produced by blasts is the primary factor for breaking or fragmenting rock mass. Nevertheless, a large amount of EE is wasted and not used for this purpose ($\sim$ 75–85%). In particular, undesirable environmental issues result from wasted EE, such as ground vibration (GV), air over-pressure, flyrock, and air pollution (e.g., dust and gases) (Armaghani et al., 2015; Kahriman et al., 2006; Mahdiyar et al., 2018; Murlidhar et al., 2020; Ozer et al., 2008). Thus, GVs have a profound impact on the environment and the areas surrounding OPMs (Fig. 1).

Many researchers have stated that GV depends on the blasting parameters and characteristics of rock mass (Faramarzi et al., 2014; Kahriman, 2002). However, rock mass factors are uncertainty parameters, and they are classified in the uncontrollable parameters in mining and blasting (Armaghani

et al., 2016; Ghasemi et al., 2012; Monjezi et al., 2011). Thus, blasting parameters are considered important in controlling the GVs induced by blasting operations in OPMs by tuning them into blast patterns (Nguyen et al., 2019a). It is noteworthy that tuning blasting parameters can reduce the adverse effects of GV, but they can also reduce the benefits of blasting operations (Afeni, 2009). Therefore, tuning blasting parameters with the reduction of GV and the improvement of the rock breaking efficiency is challenging.

Many researchers have developed, proposed, and applied state-of-the-art techniques to predict the intensity of GVs based on influential parameters (e.g., blasting parameters, characteristics of rock mass). For instance, Armaghani et al. (2015) applied two algorithms in terms of artificial intelligence (AI) to predict the GV intensity in quarry blasting sites, namely artificial neural network (ANN) and adaptive neuro–fuzzy inference system (ANFIS). Finally, they found that the fuzzy system can predict the GV intensity in quarry blasting sites with higher accuracy compared with the ANN model. Hajihassani et al. (2015) also proposed the ICA-based ANN model for predicting the intensity of GVs. In their study, the imperialist competitive algorithm (ICA) played a dominant role in improving the ANN model' accuracy. They found that the ICA significantly improved the ANN model's performance with a promising result in predicting GV. Faradonbeh

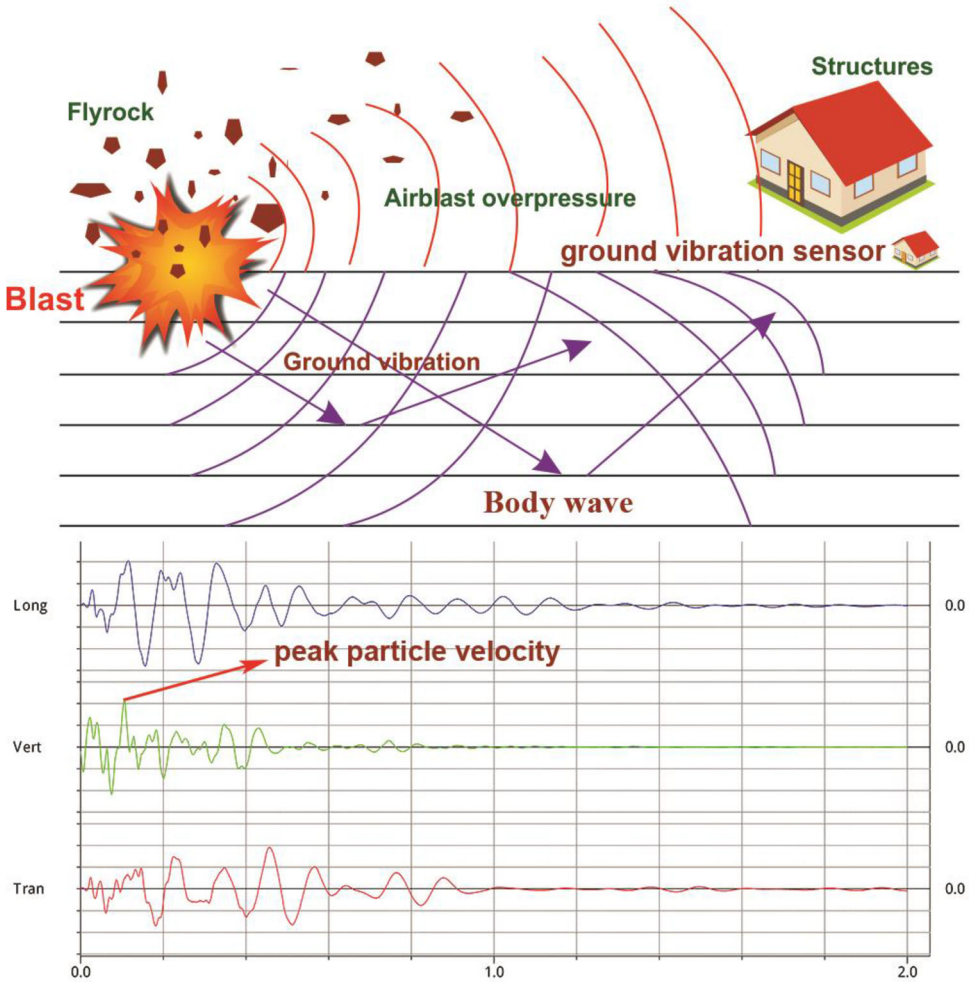


**Figure 2.** Blast-induced GV in OPMs (Nguyen et al., 2019b).

et al. (2016) approached another AI technique, namely gene expression programming (GEP), to predict the GVs in granite quarry, and their results showed that GEP is a potential model for GV prediction with acceptable accuracy (over 90%). Based on the ICA's advantages, Armaghani et al. (2018) demonstrated its feasibility in predicting GV in three quarry mines in Malaysia based on several empirical equations. Ultimately, ICA coupled with a quadratic equation was found to be the best solution in predicting GV. Similar to ICA, the genetic algorithm (GA) and particle swarm optimization algorithm (PSOA) are also robust optimization algorithms, and they were used by Yang et al. (2019) in optimizing an ANFIS model for predicting GV. The results demonstrated that the GA-based ANFIS model provides more outstanding performance than that of the PSOA-based ANFIS model, where the error decreased by 61% and the determination coefficient increased by 10%. Besides, an improved version of the PSO algorithm, namely autonomous group PSOA (abbreviated as AGPSOA), was also developed and combined with the extreme learning machine (ELM) to estimate GVs in mine blasting (Armaghani et al., 2020). The results showed that the AGPSOA–ELM model is superior to the PSOA–ELM model with a RMSE of 0.008 and a determination of coefficient ($R^2$) of 0.92. Also, based on ANN and itemset mining (IM), Amiri et al. (2020) thoroughly investigated the efficiency of a novel AI model in predicting the intensity of GVs, called the IM–NN model. Accordingly, the IM algorithm was used to extract the itemsets in a dataset and select the most appropriate itemset. Subsequently, an ANN model was trained as an optimal ANN model based on the chosen itemset. Amiri et al. (2020) found that the IM–NN model can predict GV with high accuracy, so it was proposed as a good method for predicting the GV intensity in surface mines. Moreover, based on the hybridization approach of different algorithms, Zhou et al. (2020) proposed another AI approach for predicting the intensity of GV, namely FS–RF, based on the feature selection (FS) and random forest (RF) algorithms. The FS–RF model showed a reasonably good performance with an accuracy of 90.32% in practical engineering. Using another FS algorithm, namely fuzzy Delphi (FD), Huang et al. (2020) successfully developed several hybrid models for predicting GV, such as FD–GA–ANN, FD–PSO–ANN, FD–ICA–ANN, FD–FA (firefly algorithm)–ANN, and artificial bee colony algorithm (FD–ABCA)–ANN models. Finally, the FD–FA–ANN model provided higher performance than that of the other models in predicting the intensity of GV. Based on the optimization algorithm inspired by moth–flame (MFO), Lawal et al. (2021) introduced a new model (MFO–ANN) for predicting GV, and it showed promising results (i.e., mean-squared-error (MSE) = 0.0009, $R^2$ = 0.970, VAF = 97.047). Also, two other novel hybrid intelligent models, namely grasshopper optimization algorithm (GOA)–ELM and Harris hawks optimization (HHOA)–ELM, were developed by Yu et al. (2021) to estimate the

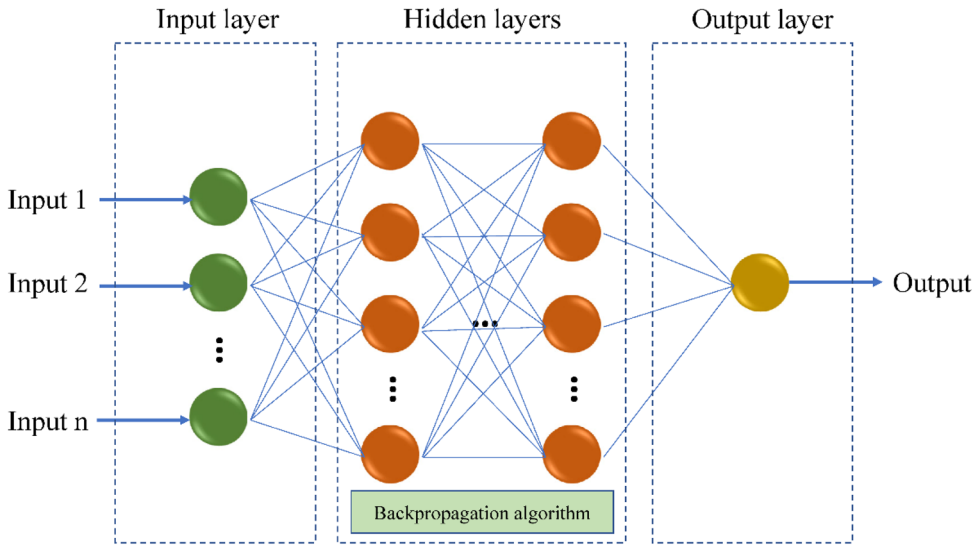


**Figure 3.** General structure of a DNN model with one output variable.

(1). Set up the initial parameter values, such as the population size n, the maximum number of iterations $t_{\max}$, the dimensions of solving problems *dim*, the upper bounds *up*, and the lower bounds lb .

(2). Generate a population of the hawks $x_i = (x_{i,1}, x_{i,2}, \ldots, x_{i,j}, \ldots x_{i,\dim})$, and calculate the fitness values $fit(x_i)$.

(3). Find the best position $x_{rabbit}$ of the population.

(4) for t=1 to $t_{\max}$

(5) Cross-border processing and evaluate the fitness value for each hawk $x_i^t$.

(6) Update the location $x_{rabbit}$ and fitness value $fit(x_{rabbit})$ of the rabbit.

(7) Calculate the decreasing energy $E_1$ of the rabbit.

(7). for i=1:*n*

(8). Calculate the escaping energy $E$ using **the following equation:**

(9). $$E = 2 * E_0 * (1 - t/t_{\max})$$

(11). if $|E| \geq 1$ then

(12). Execute exploration stage using **the following equation:**

(13). $$x_i^{t+1} = \begin{cases} x_{rand}^t - r_1 * |x_{rand}^t - 2 * r_2 * x_i^t|, & q \geq 0.5 \\ (x_{rabbit} - x_{mean}^t) - r_3 * (lb + r_4 * (ub - lb)), & q < 0.5 \end{cases}$$

(14). else if $|E| < 1$ then

(15). if $r \geq 0.5$ **and** $|E| \geq 0.5$ then

(16). Execute soft besiege using **the following equations:**

(17). $$x_i^{t+1} = \Delta x_i^t - E * |J * x_{rabbit} - x_i^t|$$

(18). $$\Delta x_i^t = x_{rabbit} - x_i^t$$

(19). else if $r \geq 0.5$ **and** $|E| < 0.5$ then

(20). Execute hard besiege using **the following equation:**

(21). $$x_i^{t+1} = x_{rabbit} - E * |\Delta x_i^t|$$

(22). else if $r < 0.5$ **and** $|E| \geq 0.5$ then

(23). Execute soft besiege with progressive rapid dives using **the following equations:**

(24). $$y = x_{rabbit} - E * |J * x_{rabbit} - x_i^t|$$

(25). $$z = y + s * levy(\dim)$$

(26). $$levy(x) = 0.01 \times \frac{u \times \sigma}{|\mu|^{\frac{1}{\beta}}}, \sigma = \left( \frac{\Gamma(1+\beta) \times \sin\left(\frac{\pi\beta}{2}\right)}{\Gamma\left(\frac{1+\beta}{2}\right) \times \beta \times 2^{\left(\frac{\beta-1}{2}\right)}} \right)^{\frac{1}{\beta}}$$

(27). $$x_i^{t+1} = \begin{cases} y, & \text{if } f(y) < f(x_i^t) \\ z, & \text{if } f(z) < f(x_i^t) \end{cases}$$

(28). else if $r < 0.5$ **and** $|E| < 0.5$ then

(29). Execute hard besiege with progressive rapid dives using **the following equations:**

(30). $$x_i^{t+1} = \begin{cases} y, & \text{if } f(y) < f(x_i^t) \\ z, & \text{if } f(z) < f(x_i^t) \end{cases}$$

(31). $$y = x_{rabbit} - E * |J * x_{rabbit} - x_{mean}^t|$$

(32). end if

(33). endif

(34). endfor

(35). end for

(36). Output the best solution $x_{rabbit}$ and its fitness value $fit(x_{rabbit})$.

**Figure 4.** Step-by-step instructions for solving an optimization problem using HHOA.

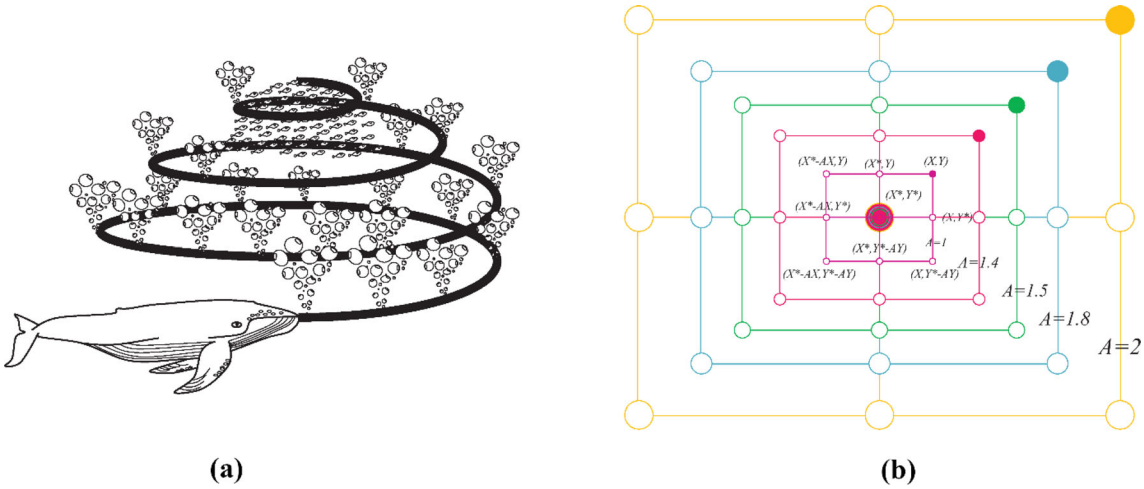


**Figure 5.** Strategies of the WOA for solving optimization problems (Mirjalili & Lewis, 2016). **a** Exploitation phase. **b** Exploration phase.

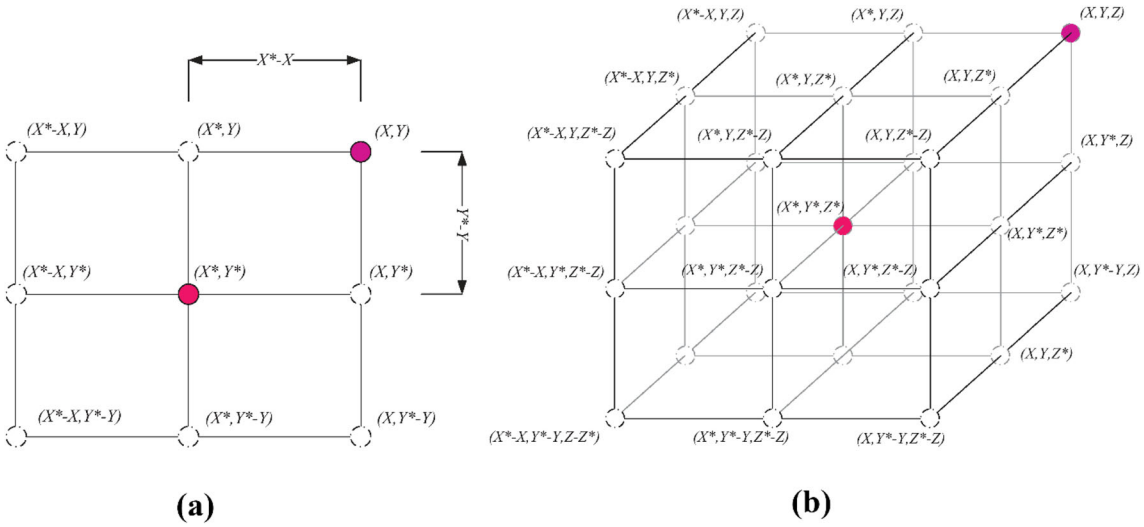


**Figure 6.** Position vectors and their next possible locations. **a** 2D problems. **b** 3D problems.

intensity of the GVs resulting from mine blasting. They found that the GOA–ELM model provides more accurate GV values compared with the HHOA–ELM model (i.e., RMSE = 2.024, $R^2$ = 0.941). Similar works can be referred to in other literature (Arthur et al., 2020; Bayat et al., 2020; Bisoyi & Pal, 2020; Ding et al., 2020; Fattahi & Hasanipanah, 2020; Mohammadi et al., 2020; Singh et al., 2020; Yang et al., 2020; Yu et al., 2020).

Although many AI techniques and efforts were proposed for predicting the GV intensity in OPM to reduce the adverse effects of mine blasts, the enhancement of AI models is still a challenge. Furthermore, the accuracies of the proposed models cannot reflect the generalized characteristics of different locations/areas. Thus, this study proposed several novel hybrid AI models based on deep neural networks (DNNs) and nature-based optimization algorithms (i.e., HHOA, whale optimization algorithm—WOA, and PSOA) to predict the GV intensity induced by mine blasting, namely HHOA–DNN, WOA–DNN, and PSOA–DNN. It is

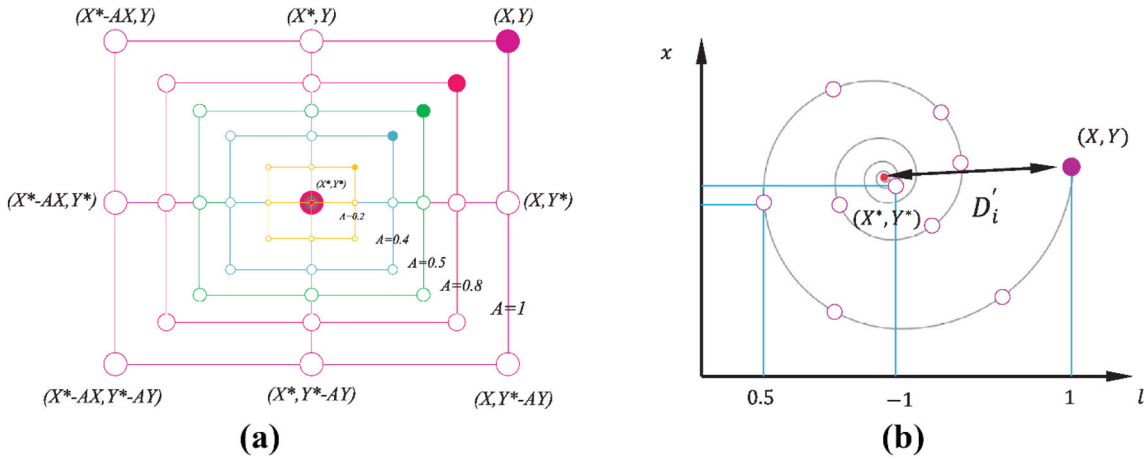


**Figure 7.** Bubble-net search mechanisms of WOA. **a** Shrinking encircling. **b** Spiral updating position.

worth mentioning that (i) DNN has not been used to predict GV in OPM, (ii) HHOA has not been applied to optimize a DNN model for predicting the intensity of GV, and (iii) HHOA, PSOA, and WOA have not been applied to continue improving a deep neural network for GV prediction. Finally, the results were compared and evaluated comprehensively in terms of GV prediction.

## MECHANISM OF BLAST-INDUCED GROUND VIBRATION

In mine blasting, after detonating an amount of explosives, the entire contact surface between rocks and explosives is considered to be simultaneously affected by gas pressure and waves. Near explosives, under the effect of gas pressure ($\sim 10^5$ kg/cm$^2$), rock is compressed and crushed, strongly deformed, and moved in a radius. The movement of the rocky particles close to explosions is propagated to the next layer of rock constituents and shock wave is formed on the rocky environment. In essence, a shock wave is a form of a compressive stress wave, and it has a much greater amplitude than that of the compressive strength of rock. Shock waves can destroy and deform rocks and also generate cracks in them.

A shock wave generated by blasting moves at ultrasonic speed and propagates to certain distances (about 5 to 6 times the explosion radius). Then, it turns into an elastic wave at a speed less than the initial one and equal to the speed at which sound waves propagate in rocky environments. After shock waves pass through rock particles, they move under the received wave energy (Duvall & Petkof, 1959). The wave amplitude value gradually decreases when away from the explosion center. Therefore, the destructive and deformed properties of the rock environment are also changed. Rock is destroyed at the areas receiving shock waves with amplitudes greater than the rock's compressive strength. Depending on the difference between a shock wave's amplitude and a rock's compressive strength, the destruction level is different. The closer to the blast center, the greater the difference between the amplitude of a shock wave and a rock's compressive strength, and the higher the rock destruction level. According to the degree of destruction, the explosive effects can be classified into zones as follows:

*Zone 1:* This area is right next to the explosives. In this area, rock is directly affected by explosive pressure (about $10^5$ kg/cm$^2$). Therefore, if the rock is soft, it is compressed to become more durable and forms a hollow chamber. However, if it is hard, it is destroyed and crumbled. In other words, this area is also referred to as the compression zone or crush zone.

*Zone 2*: The contiguous area immediately follows zone 1. This area is affected by a smaller shock wave amplitude than that of Zone 1. However, it is still sufficient to destroy rock structures and form fractures. This area is also known as the fracture zone.

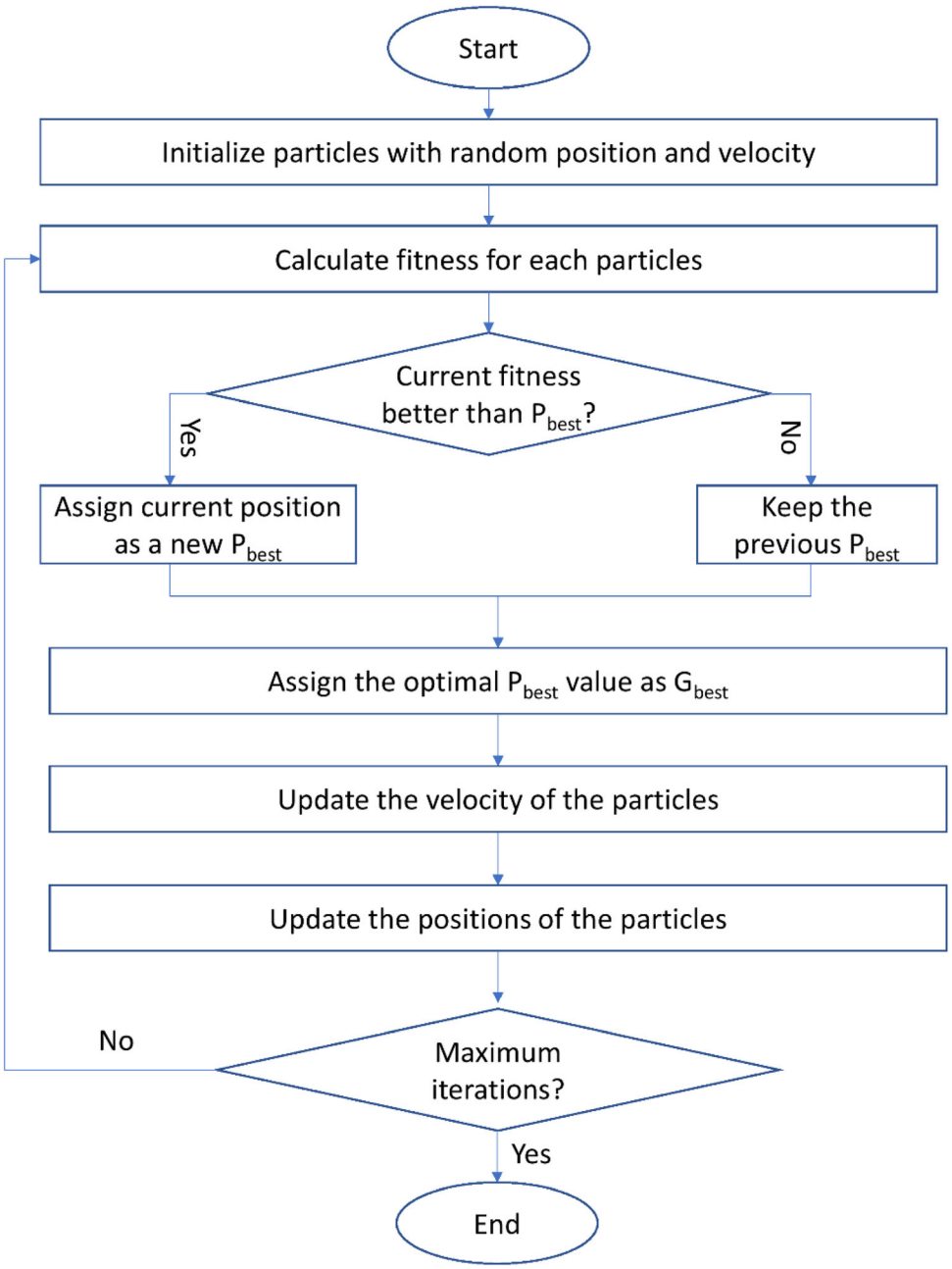


**Figure 8.** Flowchart of the PSOA for optimization problems.

*Zone 3:* The contiguous area immediately follows zone 2. In this area, the shock wave's amplitude is less than the rock's compressive strength and is not enough to destroy or crack rock. At that time, the shock wave turns into an elastic oscillating wave in the rocky environment and only causes ground vibrations. Therefore, it is called blast-induced ground vibration. This area is also known as the vibration zone. An illustration of blast-induced GV is shown in Figure 2. To measure the intensity of GV, the peak particle velocity (Fig. 2) is used as a crucial parameter in mine blasting.

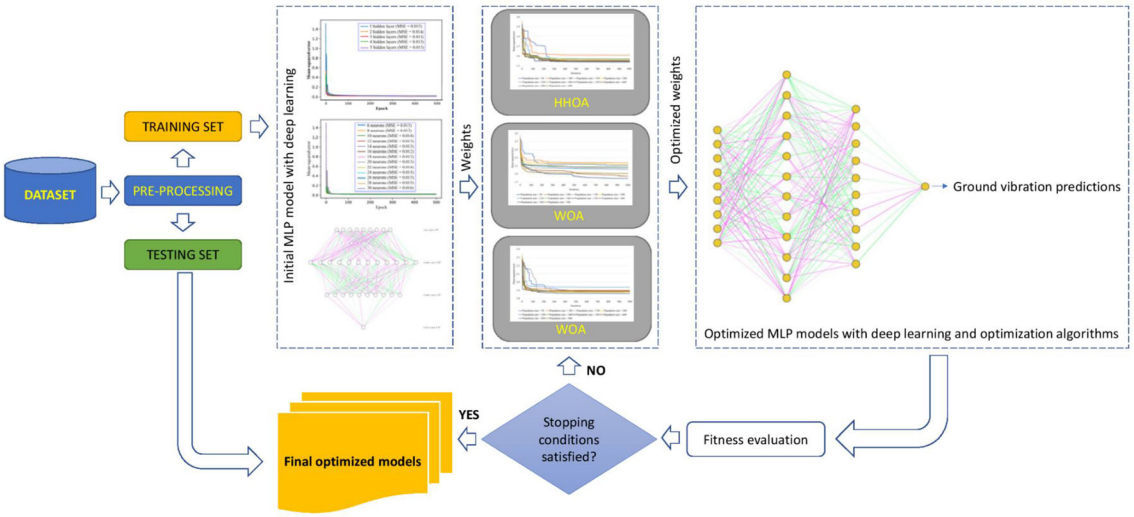


**Figure 9.** Proposed framework of the HHOA–DNN, WOA–DNN, and PSOA–DNN models for predicting GV.

## BACKGROUND KNOWLEDGE FOR INTELLIGENT SYSTEMS

### Deep Neural Network

In data mining and machine learning, ANN is well known as a robust intelligent technique that has been successfully applied in industry for decades. In ANN, there are many types of networks, and they are designed/developed based on the human nervous system, such as the radial basis function, modular, recurrent, feedforward, convolutional, Korhonen self-organizing, and long-short term memory neural networks (Maleki et al., 2020; Senthil Kumar et al., 2005; Yegnanarayana, 2006; Zou et al., 2008). Of those, multi-layer perceptron (MLP) is a type of feedforward neural network and is the foundation of deep learning for improving the model performance of ANNs (Brownlee, 2018). MLP uses the backpropagation algorithm for training predictive models as supervised learning techniques, and it can effectively solve nonlinear problems. An MLP network topology with multiple hidden layers and deep learning techniques is also referred to as a DNN.

A DNN consists of at least three layers: an input layer, one or multiple hidden layers, and an output layer (Fig. 3). In the input layer, neurons act as receivers and provide information to the hidden layer(s). Next, the neurons in the hidden layer(s) act as processers and learners. They implement a calculation between neurons and assign the results as weights between them. Finally, weights are processed and transferred to the output layer, and the outcomes are predicted and displayed.

Deep learning techniques aim at improving the efficiency of DNNs, and they can be applied to predicting GV. In this sense, the performance of a DNN model can be improved by the configuration of capacity, gradient precision, loss functions, learning speed, to name a few (Salman et al., 2015; Goodfellow et al., 2016; Garcia-Garcia et al., 2018; Han et al., 2018). In this study, several deep learning techniques were used to design and develop a DNN model to achieve good predictive modeling performance in GV prediction.

### Harris Hawks Optimization Algorithm (HHOA)

HHOA is a nature-inspired optimization algorithm that was developed by Heidari et al. (2019). It closely mimics the actions of Harris hawks in nature and is often used to solve complex optimization problems with high performance (Beskirli & Dağ, 2020; Gölcük & Ozsoydan, 2021; Heidari et al., 2019). The significant advantage of HHOA is that it can solve optimization problems without gradient. To solve optimization problems, HHOA applies a hunting algorithm with two stages: exploration and exploitation. In the exploration stage, Harris hawks perch on random trees or their previous locations to

explore the locations of prey using their bright eyes. Subsequently, they pounce preys using their skills (called besieges), including soft besiege and hard besiege. Progressive rapid dives can also be applied to optimize the hawks' purposes and avoid the escape of prey. The pseudocode of HHOA is shown in Figure 4. Further details of HHOA can be found in previous literature (Bairathi & Gopalani, 2018; Heidari et al., 2019; Moayedi et al., 2019; Munagala & Jatoth, 2020; Zhang et al., 2020a, 2020b).

## Whale Optimization Algorithm

Like HHOA, WOA is also a nature-inspired optimization algorithm, and it was designed based on the hunting mechanism of humpback whales (Mirjalili & Lewis, 2016). They use a unique strategy to hunt prey called bubble-net (Fig. 5a), where they encircle and then attack their prey. Subsequently, they randomly search for prey according to the locations of individual humpback whales (Fig. 5b).

In contrast to HHOA, WOA implements the exploitation phase before the exploration phase. In

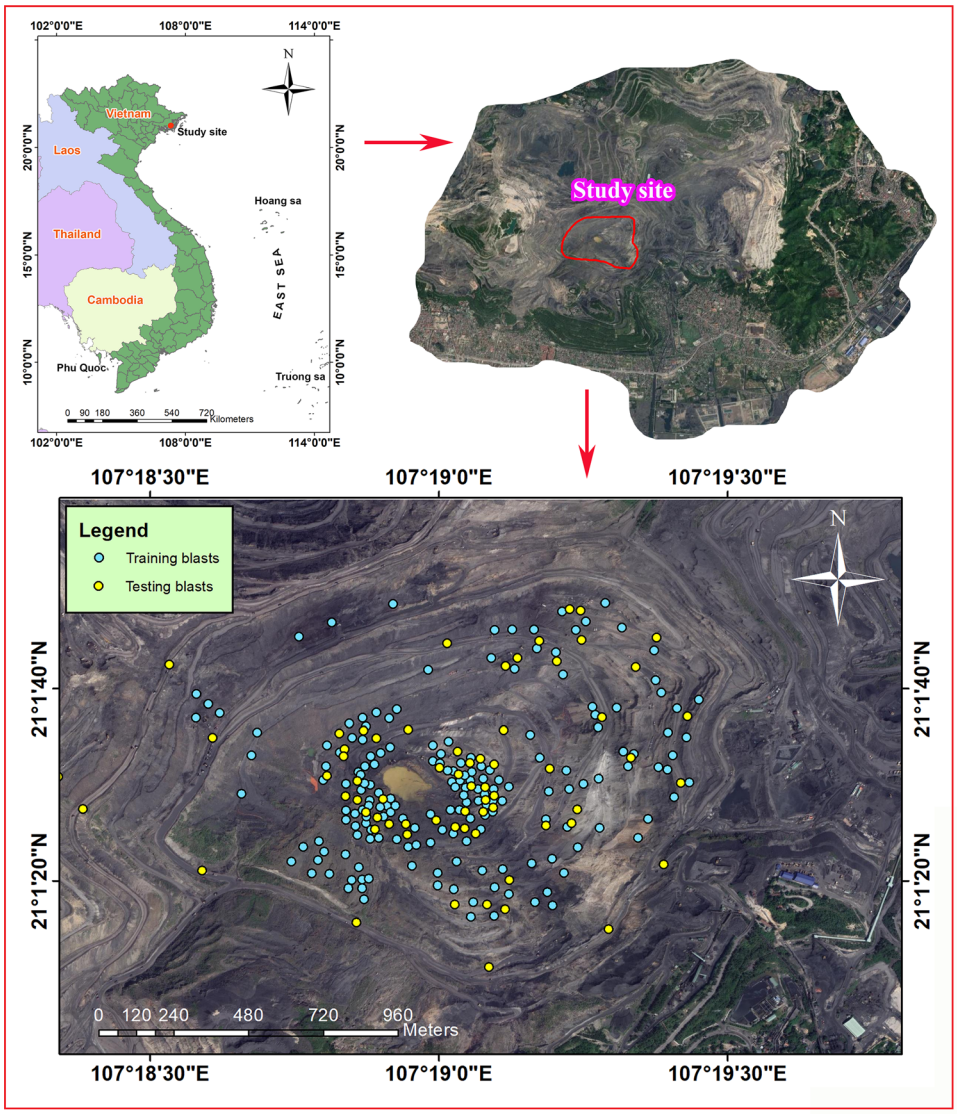


**Figure 10.** Study site and locations of blasting events.

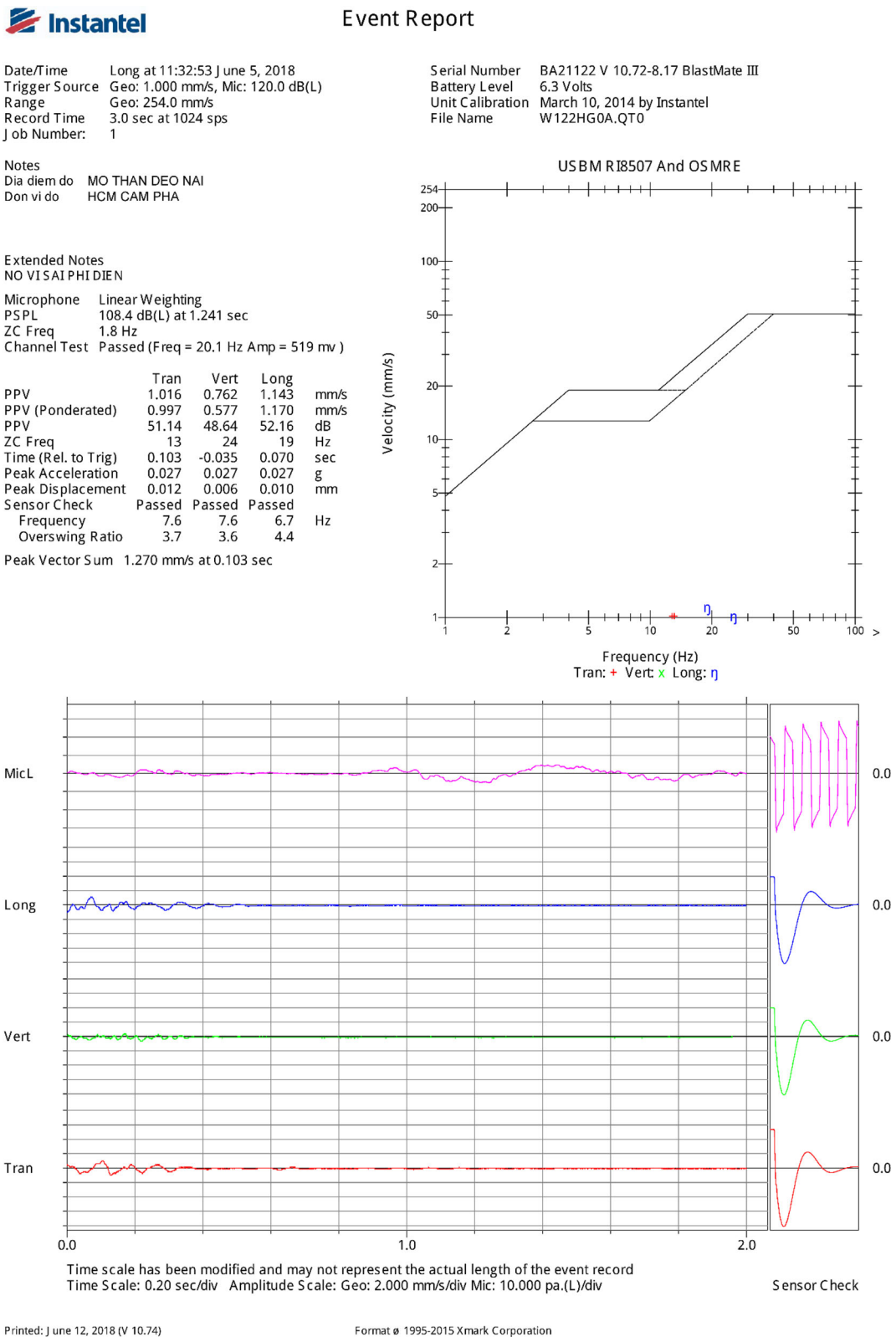


**Figure 11.** An event report of GVs induced by mine blasting at the study site.

the encircling prey stage of the exploitation phase, WOA searches a space with 2D or 3D, as shown in Figure 6. Afterward, it applies two bubble-net search mechanisms, such as the shrinking encircling mechanism and spiral updating position, to attack prey (Fig. 7). Finally, it searches for prey in the exploration phase toward a better solution, and it can perform a global search to achieve this purpose. Further details of WOA can be found in previous literature (Chen et al., 2020; Krithiga & Ilavarasan, 2020; Li & He, 2020; Mirjalili & Lewis, 2016; Singh & Khamparia, 2020; Yan et al., 2021; Zeng et al., 2021).

### Particle Swarm Optimization Algorithm

PSOA is distinguished as a flexible optimization algorithm, and it was proposed by Kennedy and Eberhart (1995). Due to its flexibility, PSOA has been developed and enhanced with many versions to solve different optimization problems (Cao et al., 2017; Molaei et al., 2021; Qi, 2021; Qian et al., 2020; Radha & Gopalakrishnan, 2020; Shankar & SaravanaKumar, 2020; Wang et al., 2021). It is considered a robust optimization algorithm for global search, and it is easy to implement. The concept of PSOA is based on the behavior of particle swarms and their information exchange mechanism. They keep exchanging information and updating their feature space positions to find a better place as a global optimization. The flowchart of PSOA is illustrated in Figure 8, and its in-depth details can be found in previous literature (Bratton & Kennedy, 2007; Clerc, 2010; Du & Swamy, 2016; Kiranyaz et al., 2014; Lazinica, 2009; Poli et al., 2007). Although the PSOA was developed in 1995, its advantages and convenience are still appropriate in many areas, especially in engineering applications. Therefore, it was selected as an optimizer to improve the DNN's performance in predicting GV.

### Hybridization of Intelligent Models

Based on the background knowledge of DNNs and other optimization algorithms, this study proposed a DNN model framework based on optimizers of HHOA, WOA, and PSOA to predict GV, namely HHOA–DNN, WOA–DNN, and PSOA–DNN (Fig. 9). Accordingly, deep learning techniques were first applied to develop the initial MLP model. Then, the HHOA, WOA, and PSOA optimizers were used to train the developed DNN model, aiming to improve the DNN model's accuracy through the network's weights.

In the first step of the framework, deep learning techniques were used to design an optimal DNN model structure. To this end, a number of populations of the optimizers were used to obtain the optimal values of weights to achieve the best performance of the DNN model. The optimizers' searching process was repeated with many iterations to get the best performance since the optimizers' chaotic and different performances were obtained in each iteration. To evaluate the performance of the hybrid models in the optimization progress, MSE was used as an objective function. Finally, the optimized hybrid models were determined and applied to predict GVs.

## STUDY SITE AND DATA ACQUISITION

Once the framework of the hybrid models was determined and proposed, the Deo Nai open-pit coal mine (Vietnam) was selected as a case study site to evaluate the proposed framework's performance. This mine is one of the biggest open-pit coal mines in Vietnam, and it is located in northern Vietnam, as shown in Figure 10. This mine's surroundings are other mines, structures, and residential areas with distances in the range of 100–200 m.

In this mine, the hardness of rock mass is 12, according to Protodiakonov's coefficient (Nguyen et al., 2018). Thus, the blasting method is the most common and valuable method in this mine to fragment the overburden and original rocks around coal seams. However, as mentioned above, blasting operations cause many side effects, especially GVs. Therefore, aiming at preventing the side effects of GV, this study focused on the GV intensity induced by blasting operations and on developing novel hybrid models for predicting GV with high accuracy.

As explained by previous researchers, blast-induced GVs are affected by two groups of parameters: blasting parameters (controllable parameters) and geological parameters (uncontrollable parameters) (Amiri et al., 2016; Hasanipanah et al., 2015, 2017; Himanshu et al., 2018). However, due to the uncertainty characteristics as well as high cost of collecting and surveying geological and geophysical parameters, these parameters are rarely used to predict blast-induced GV (Kumar et al., 2016; Na-

teghi, 2011). Instead, blasting parameters are used to predict blast-induced GVs, and the results differ based on each region's geological and geophysical conditions. Therefore, herein, 229 blasting events were collected with eight blasting parameters recorded: explosive charge per blast (ECPB), number of groups, time delay (TL), hole length, burden (B), spacing (S), stemming (ST), powder factor (PF)), distances (D), and GV intensity. Of those, eight blasting parameters were recorded from the blasting patterns, where a GPS receiver measured the distances, and the GV intensity values were recorded by a Micromate (Instantel, Canada). It is worth noting that each GV intensity value corresponds to a distance and a set of blasting parameters (i.e., blasting patterns). Figure 11 illustrates an event report of GVs induced by mine blasting at the study site. Finally, the mentioned blasting parameters were used as inputs and outputs for predicting GVs in this study, and they are summarized in Table 1. The study site and locations of the blasting events are illustrated in Figure 10.

Before developing the predictive models, the correlation coefficients between the variables were computed and evaluated using a correlation matrix to show the relationship between the variables and determine which variables should be removed. Table 2 shows the relationship between the variables used through the correlation coefficients. Based on the correlation statistics, it can be seen that all the variables poorly correlate with each other (correlation coefficient is smaller than 0.75) and that they should be used to predict GV as independent variables.

**Table 1.** Summary statistics of the dataset attributes

| Category | ECPB | NG | TD | HL | B |
|---|---|---|---|---|---|
| Min | 305 | 2 | 17 | 12.4 | 6.3 |
| 1st Qu | 2526 | 2 | 17 | 13.5 | 7.1 |
| Median | 3326 | 3 | 25 | 14.2 | 7.7 |
| Mean | 3202 | 3.319 | 27.38 | 14.36 | 7.616 |
| 3rd Qu | 3919 | 4 | 42 | 15 | 8.2 |
| Max | 6043 | 5 | 42 | 16.7 | 8.5 |
| Category | S | ST | PF | D | PPV |
| Min | 6.2 | 4.6 | 0.32 | 180 | 2.14 |
| 1st Qu | 7 | 5.9 | 0.39 | 322.7 | 8.24 |
| Median | 7.6 | 6.5 | 0.42 | 402 | 12.58 |
| Mean | 7.451 | 6.448 | 0.4131 | 433.1 | 12.61 |
| 3rd Qu | 7.8 | 7 | 0.44 | 523 | 16.14 |
| Max | 8.2 | 7.5 | 0.5 | 726 | 28.63 |

## RESULTS AND DISCUSSION

To develop the HHOA–DNN, WOA–DNN, and PSOA–DNN models for predicting GV in this study, the prediction architecture in Figure 9 was applied. Accordingly, the dataset was split into two parts. The first part was a randomly selected training dataset with 70% of the whole dataset ($\sim$ 160 blasting events), and the second part comprising the remaining 30% ($\sim$ 69 blasting events) was used to validate the developed models. It is worth mentioning that many previous researchers recommended this ratio to ensure the generalization of predictive models (Liu & Cocea, 2017; Setiawan et al., 2020; Sulaiman et al., 2011). Subsequently, the datasets were processed before the development of the stage of models to avoid over-fitting or under-fitting problems as well as improve the accuracy of the GV predictive models. The min–max scaling

**Table 2.** Correlation matrix of the dataset used

| | ECPB | NG | TD | HL | B | S | ST | PF | D | GV |
|---|---|---|---|---|---|---|---|---|---|---|
| ECPB | 1 | 0.169 | − 0.358 | 0.453 | 0.052 | 0.235 | − 0.270 | 0.461 | − 0.648 | 0.623 |
| NG | 0.169 | 1 | − 0.064 | 0.148 | 0.089 | 0.151 | 0.069 | − 0.005 | − 0.113 | 0.143 |
| TD | − 0.358 | − 0.064 | 1 | − 0.109 | − 0.001 | − 0.118 | − 0.078 | − 0.416 | 0.273 | − 0.367 |
| HL | 0.453 | 0.148 | − 0.109 | 1 | − 0.040 | 0.133 | − 0.167 | 0.007 | − 0.422 | 0.429 |
| B | 0.052 | 0.089 | − 0.001 | − 0.040 | 1 | 0.697 | 0.591 | 0.256 | 0.251 | 0.018 |
| S | 0.235 | 0.151 | − 0.118 | 0.133 | 0.697 | 1 | 0.660 | 0.241 | 0.091 | 0.269 |
| ST | − 0.270 | 0.069 | − 0.078 | − 0.167 | 0.591 | 0.660 | 1 | 0.058 | 0.596 | − 0.265 |
| PF | 0.461 | − 0.005 | − 0.416 | 0.007 | 0.256 | 0.241 | 0.058 | 1 | − 0.317 | 0.441 |
| D | − 0.648 | − 0.113 | 0.273 | − 0.422 | 0.251 | 0.091 | 0.596 | − 0.317 | 1 | − 0.571 |
| GV | 0.623 | 0.143 | − 0.367 | 0.429 | 0.018 | 0.269 | − 0.265 | 0.441 | − 0.571 | 1 |

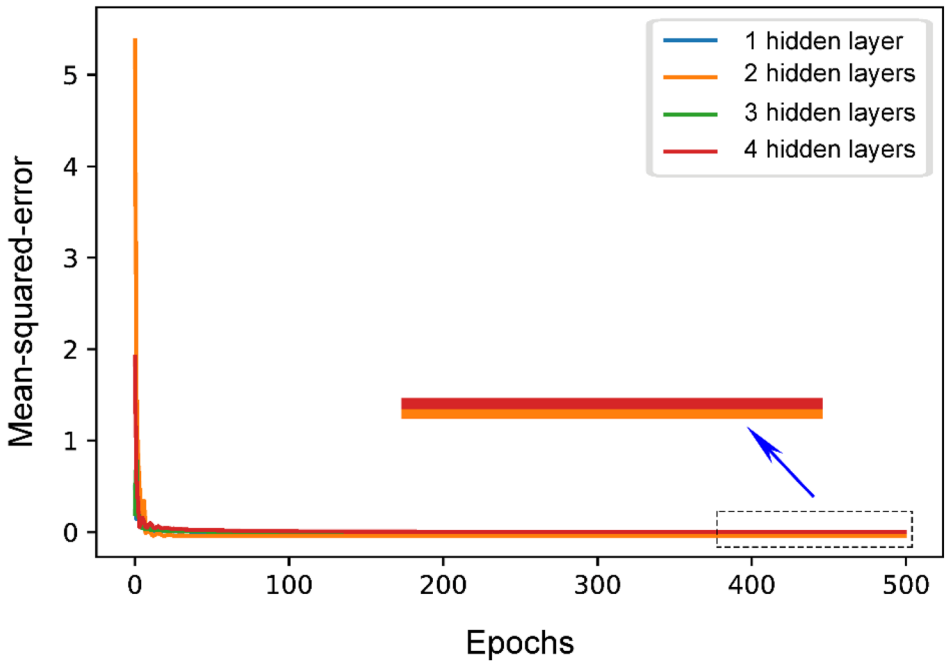


(a)

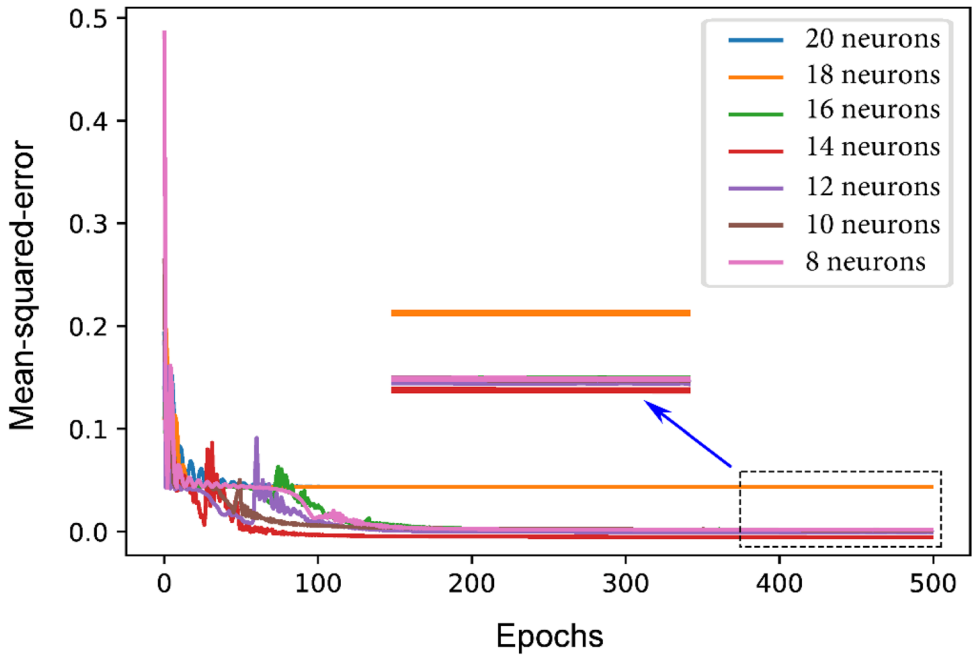


(b)

**Figure 12.** Selection of the best DNN model structure using deep learning techniques. **a** Selection of the number of hidden layers. **b** Selection of the number of neurons.

method was applied to normalize the dataset to a 0–1 range using the following equation:

$$X_{sc} = \frac{X - X_{min}}{X_{max} - X_{min}}. \quad (1)$$

Once the dataset was well processed, the training dataset was used to develop a DNN model. However, it is very challenging to select the best DNN model structure, including the number of hidden layers and number of neurons/nodes in each hidden layer. Therefore, deep learning techniques were applied to select the best DNN model network, including ''he uniform'' kernel initializer, ''relu'' activation, and the stochastic gradient descent optimizer, with a learning rate of 0.1, a momentum of 0.85, a decay of 0.0001, a batch size of 160, and

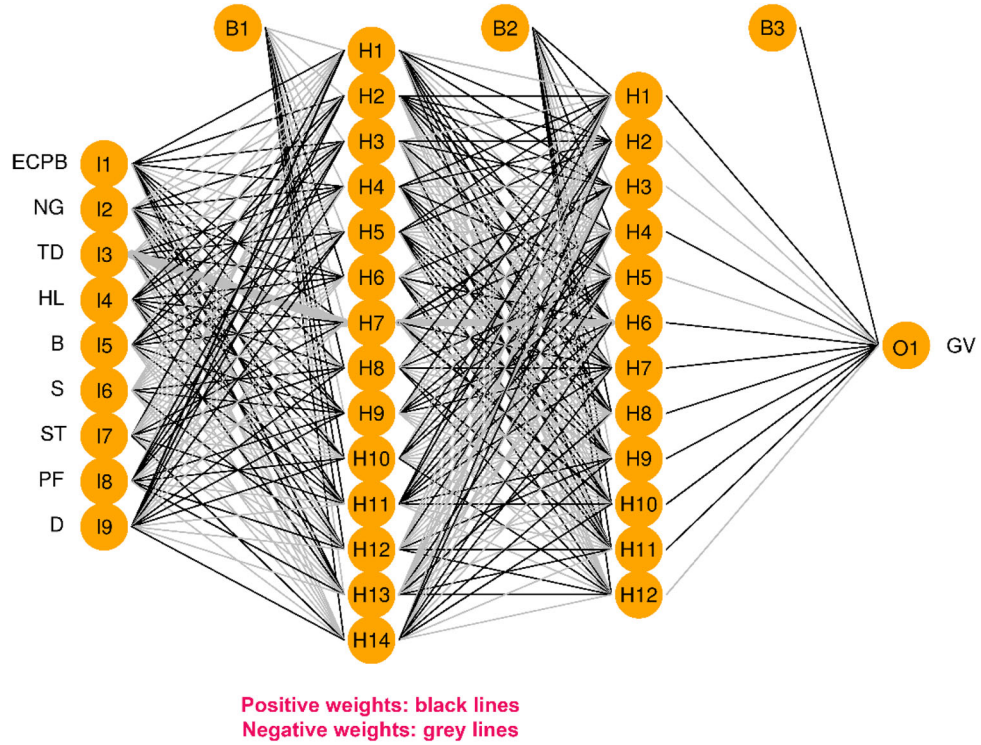


**Figure 13.** Selected DNN model for predicting GVs.

**Table 3.** Parameters of the optimizers for optimization of the MLP model

| Parameters | Optimization algorithms | | |
|---|---|---|---|
| | HHOA | WOA | PSOA |
| Number of populations | 50–500 | 50–500 | 50–500 |
| Iterations | 1000 | 1000 | 1000 |
| Minimum of the distance control parameter | – | 0 | – |
| Maximum of the distance control parameter | – | 2 | – |
| Nonlinear adjust factor | – | 0.7 | – |
| Minimum weight of the bird | – | – | 0.4 |
| Maximum weight of the bird | – | – | 0.9 |
| The effects of local and global optimization | – | – | 1.2 |

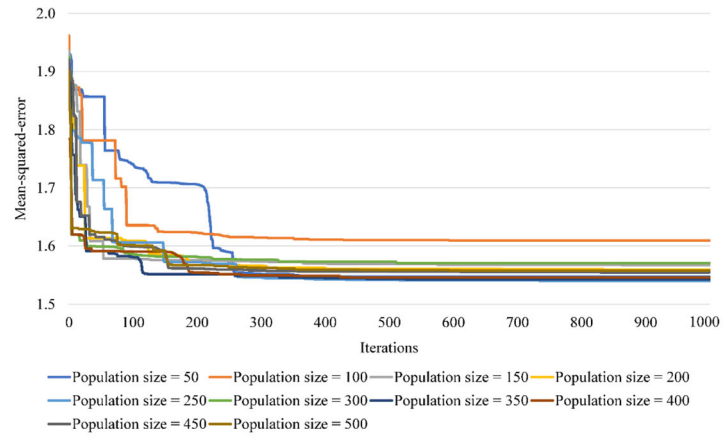


**(a)**

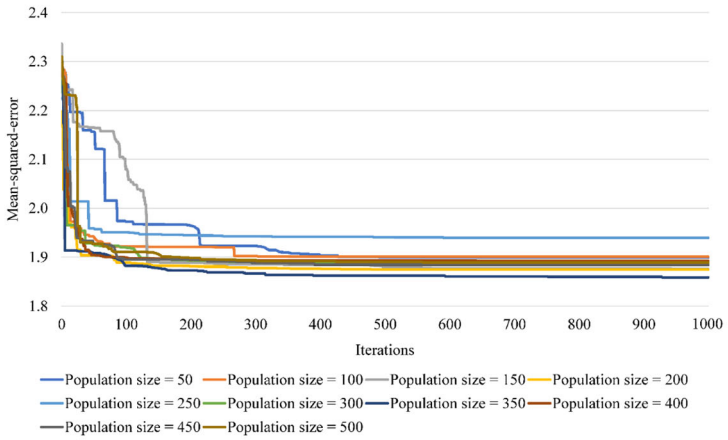


**(b)**

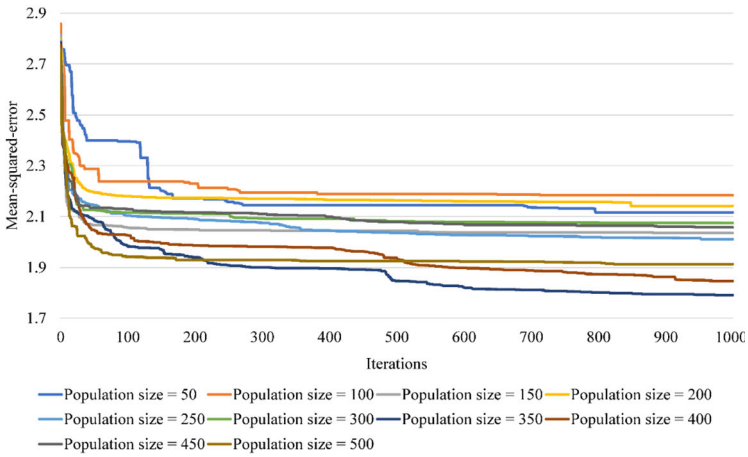


**(c)**

**Figure 14.** Performances of the DNN model optimized by different algorithms: **a** HHOA optimizer; **b** PSOA optimizer; **c** WOA optimizer.

epochs of 500. The DNN model's performance with different structures was evaluated using MSE, as described in Eq. 2, and the results are shown in Figure 12.

$$\mathrm{MSE} = \sum_{i=1}^{n} \left(GV_{\mathrm{measured}} - GV_{\mathrm{predicted}}\right)^2 \quad (2)$$

From the performances shown in Figure 12, the deep learning techniques indicated that the best DNN model structure that should be used is DNN 9-14-12-1. In other words, the best DNN model for predicting GVs has two hidden layers with 14 neurons in the first hidden layer and 12 neurons in the second hidden layer, as shown in Figure 13. It is worth noting that the values of the weights are represented by the thickness of the lines (black and gray lines) in Figure 13.

Once the DNN model's best structure was designed, the HHOA, WOA, and PSOA were embedded into the DNN model to optimize its weights, aiming at reducing the network error. The optimizer parameters (i.e., HHOA, WOA, and PSOA) are set up in Table 3. Later on, these optimizers optimized the DNN model weights, and their performance is displayed in Figure 14.

Based on the performances of the DNN model under the optimization of different algorithms, it can be observed that the HHOA–DNN model provided the best performance with a number of populations of 250 and 829 iterations (i.e., MSE = 1.540). However, the numbers of populations and iterations of the WOA–DNN model (i.e., MSE = 1.791) are 350 and 997, and those of the PSOA–DNN model (i.e., MSE = 1.859) are 350 and 929.

Based on the performances of the DNN model under the optimization of different algorithms, it can be observed that the HHOA–DNN model provided the best performance with a number of populations of 250 and 829 iterations (i.e., MSE = 1.540). However, the numbers of populations and iterations of the WOA–DNN model (i.e., MSE = 1.791) are 350 and 997, and those of the PSOA–DNN model (i.e., MSE = 1.859) are 350 and 929.

Once the GV predictive models were well developed, their results were computed and evaluated using various performance indices, such as MSE, RMSE, $R^2$, mean absolute percentage error (MAPE), and variance accounted for (VAF) using Eqs. 2–6. Finally, the obtained results were computed on both training and testing phases, as shown in Table 4. It is worth mentioning that the color scaling method was also used to highlight and classify the models based on their performances.

$$\mathrm{RMSE} = \sqrt{\frac{\sum_{i=1}^{n} \left(GV_{\mathrm{measured}} - GV_{\mathrm{predicted}}\right)^2}{n}} \quad (3)$$

$$\mathrm{MAPE} = \frac{100\%}{n} \sum_{i=1}^{n} \left| \frac{GV_{\mathrm{measured}} - GV_{\mathrm{predicted}}}{GV_{\mathrm{measured}}} \right| \quad (4)$$

$$\mathrm{VAF} = \left(1 - \frac{\mathrm{var}\left(GV_{\mathrm{measured}} - GV_{\mathrm{predicted}}\right)}{\mathrm{var}\left(GV_{\mathrm{predicted}}\right)}\right) \times 100 \quad (5)$$

$$R^2 = 1 - \frac{\sum_{i=1}^{n} \left(GV_{\mathrm{measured}} - GV_{\mathrm{predicted}}\right)^2}{\sum_{i=1}^{n} \left(GV_{\mathrm{measured}} - GV_{\mathrm{mean}}\right)^2} \quad (6)$$

As computed and shown in Table 4, the proposed hybrid models based on swarm-based optimization algorithms and deep neural networks provided better performances than those of the DNN model without optimization even though deep learning techniques have been applied DNN model. Of those, the hybrid model HHOA–DNN provided the best performance with the highest accuracy and the lowest error on both training and testing phases, followed by the PSOA–DNN, and WOA–DNN

**Table 4.** Results of the models for predicting GVs in mine blasting

| Model | Training | | | | | Testing | | | | |
|---|---|---|---|---|---|---|---|---|---|---|
| | MSE | RMSE | MAPE | VAF | $R^2$ | MSE | RMSE | MAPE | VAF | $R^2$ |
| DNN | 1.937 | 1.397 | 0.094 | 92.611 | 0.926 | 2.897 | 1.702 | 0.152 | 91.444 | 0.915 |
| HHOA–DNN | 1.540 | 1.241 | 0.088 | 94.126 | 0.941 | 2.361 | 1.537 | 0.123 | 93.015 | 0.930 |
| PSOA–DNN | 1.859 | 1.364 | 0.102 | 92.907 | 0.929 | 2.513 | 1.585 | 0.126 | 92.696 | 0.928 |
| WOA–DNN | 1.791 | 1.338 | 0.089 | 93.618 | 0.932 | 2.695 | 1.642 | 0.115 | 92.160 | 0.922 |

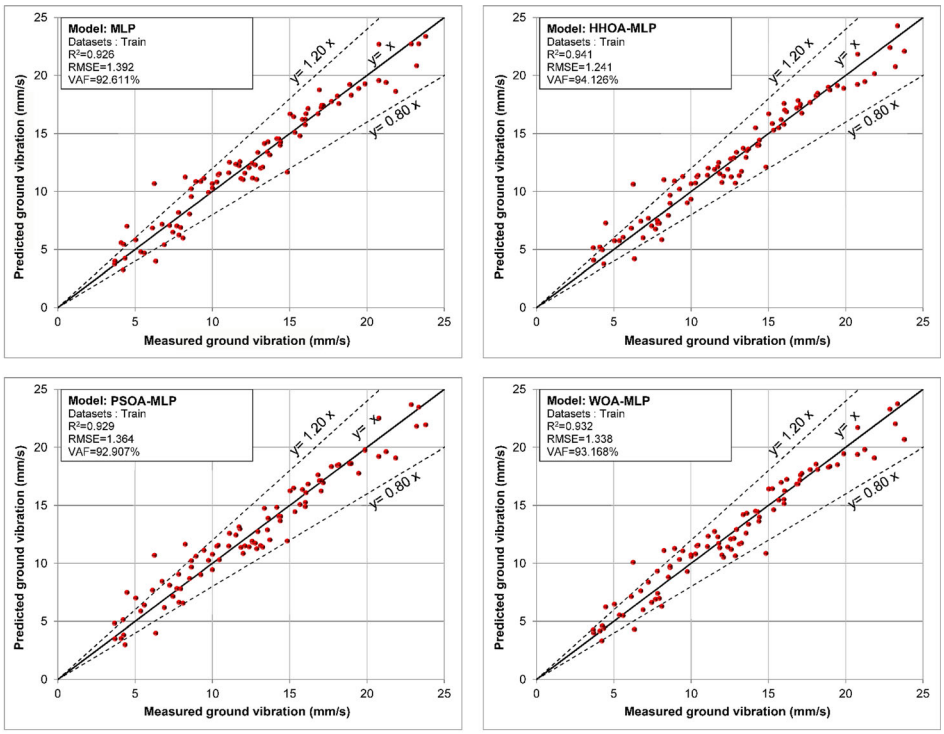


**(a)**

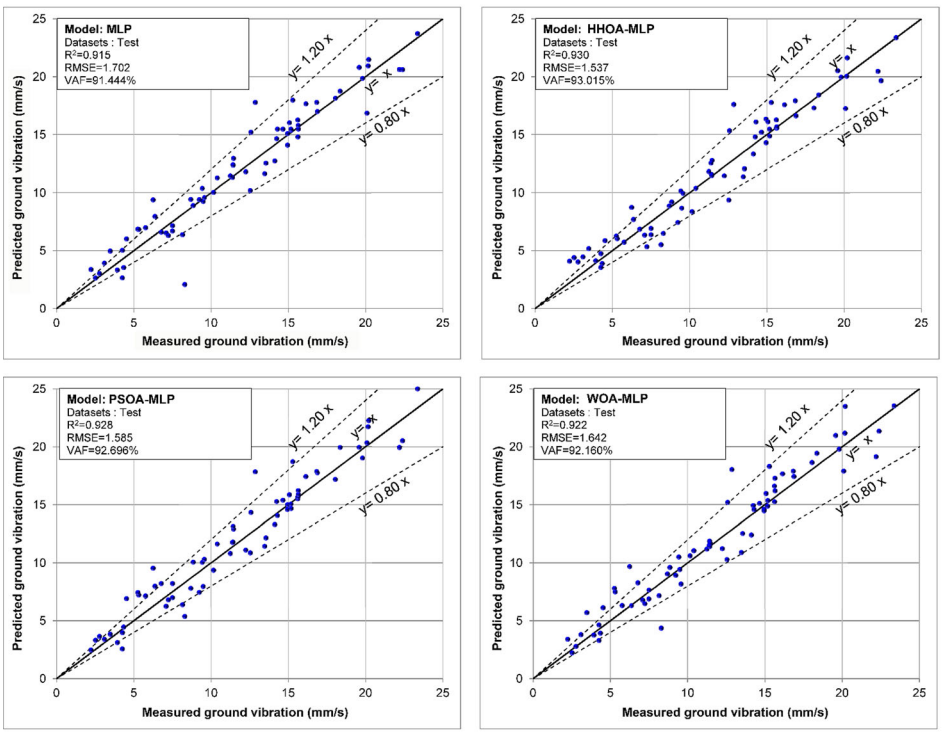


**(b)**

**Figure 15.** Relationships between the measured and predicted GVs. **a** Training correlation. **b** Testing correlation.

**Table 5.** Results of the DNN-based models on the testing dataset

| No. | Actual | DNN | HHOA–DNN | PSOA–DNN | WOA–DNN | No. | Actual | DNN | HHOA–DNN | PSOA–DNN | WOA–DNN |
|---|---|---|---|---|---|---|---|---|---|---|---|
| 1 | 11.42 | 12.41 | 11.59 | 11.80 | 11.88 | 36 | 12.25 | 11.81 | 11.46 | 11.10 | 11.23 |
| 2 | 11.45 | 12.95 | 12.77 | 12.92 | 11.70 | 37 | 15.64 | 15.48 | 15.57 | 15.89 | 16.19 |
| 3 | 7.11 | 6.54 | 6.35 | 6.25 | 6.79 | 38 | 5.32 | 6.84 | 6.04 | 7.24 | 7.50 |
| 4 | 4.35 | 3.54 | 3.89 | 4.44 | 3.92 | 39 | 12.85 | 17.79 | 17.61 | 17.84 | 18.04 |
| 5 | 23.38 | 23.73 | 23.37 | 25.00 | 23.52 | 40 | 9.57 | 9.59 | 9.95 | 10.32 | 8.18 |
| 6 | 15.60 | 16.26 | 16.27 | 15.51 | 16.60 | 41 | 14.94 | 14.09 | 14.30 | 14.99 | 14.48 |
| 7 | 13.56 | 12.53 | 12.06 | 12.15 | 12.54 | 42 | 11.40 | 11.33 | 12.54 | 11.78 | 11.50 |
| 8 | 12.59 | 15.21 | 15.34 | 14.34 | 15.20 | 43 | 5.26 | 6.86 | 6.26 | 7.43 | 7.80 |
| 9 | 18.05 | 18.13 | 17.30 | 17.18 | 18.64 | 44 | 11.24 | 11.47 | 11.81 | 10.81 | 11.19 |
| 10 | 5.75 | 6.98 | 5.73 | 7.14 | 6.31 | 45 | 15.08 | 16.02 | 16.11 | 15.86 | 15.96 |
| 11 | 2.53 | 2.65 | 4.41 | 3.32 | 2.23 | 46 | 22.38 | 20.60 | 19.66 | 20.52 | 21.34 |
| 12 | 22.20 | 20.62 | 20.46 | 19.93 | 19.14 | 47 | 6.36 | 7.96 | 7.69 | 7.97 | 6.31 |
| 13 | 3.48 | 4.96 | 5.17 | 3.83 | 5.70 | 48 | 4.25 | 2.65 | 3.55 | 2.57 | 3.30 |
| 14 | 15.28 | 17.97 | 17.78 | 18.71 | 18.30 | 49 | 14.24 | 14.64 | 14.80 | 15.27 | 14.92 |
| 15 | 9.50 | 9.25 | 8.68 | 7.98 | 9.43 | 50 | 18.37 | 18.75 | 18.42 | 19.94 | 19.44 |
| 16 | 8.30 | 2.07 | 6.50 | 5.36 | 4.35 | 51 | 8.14 | 6.39 | 5.53 | 6.40 | 7.17 |
| 17 | 13.49 | 11.65 | 11.39 | 11.43 | 10.89 | 52 | 16.14 | 17.66 | 17.57 | 17.43 | 17.66 |
| 18 | 16.88 | 16.99 | 16.62 | 17.76 | 17.42 | 53 | 7.24 | 6.31 | 5.35 | 6.81 | 6.48 |
| 19 | 7.51 | 6.71 | 6.92 | 6.99 | 6.89 | 54 | 4.52 | 6.01 | 5.87 | 6.91 | 6.12 |
| 20 | 19.80 | 19.85 | 19.97 | 19.03 | 19.79 | 55 | 14.30 | 15.47 | 16.09 | 14.07 | 14.59 |
| 21 | 15.63 | 14.79 | 15.55 | 15.67 | 15.25 | 56 | 15.17 | 15.47 | 15.48 | 15.06 | 14.86 |
| 22 | 16.85 | 17.78 | 17.92 | 17.87 | 17.88 | 57 | 20.16 | 20.93 | 20.04 | 21.72 | 21.16 |
| 23 | 14.95 | 15.09 | 16.34 | 14.59 | 14.60 | 58 | 15.65 | 15.80 | 15.67 | 16.22 | 17.27 |
| 24 | 8.85 | 8.91 | 9.20 | 10.07 | 9.61 | 59 | 3.93 | 3.34 | 4.13 | 3.10 | 3.76 |
| 25 | 12.56 | 10.20 | 9.37 | 10.86 | 10.30 | 60 | 11.43 | 12.35 | 11.49 | 13.15 | 11.41 |
| 26 | 28.63 | 22.21 | 23.88 | 23.38 | 23.40 | 61 | 10.16 | 10.03 | 8.37 | 9.37 | 10.62 |
| 27 | 8.70 | 9.43 | 8.87 | 7.81 | 9.05 | 62 | 20.08 | 16.85 | 17.24 | 20.35 | 17.90 |
| 28 | 19.57 | 20.79 | 20.51 | 19.96 | 20.97 | 63 | 9.24 | 9.41 | 7.44 | 7.47 | 8.92 |
| 29 | 20.20 | 21.48 | 21.63 | 22.26 | 23.48 | 64 | 3.10 | 3.92 | 4.46 | 3.40 | 3.80 |
| 30 | 14.13 | 12.73 | 13.32 | 13.31 | 12.40 | 65 | 7.50 | 7.15 | 6.39 | 8.22 | 7.66 |
| 31 | 15.20 | 15.38 | 14.87 | 14.67 | 15.36 | 66 | 14.67 | 15.48 | 15.21 | 15.39 | 15.11 |
| 32 | 10.41 | 11.29 | 10.38 | 11.63 | 11.05 | 67 | 2.77 | 3.03 | 4.03 | 3.64 | 2.78 |
| 33 | 9.44 | 10.39 | 10.16 | 10.05 | 10.51 | 68 | 6.25 | 9.39 | 8.74 | 9.53 | 9.68 |
| 34 | 2.25 | 3.37 | 4.10 | 2.47 | 3.40 | 69 | 6.78 | 6.60 | 6.86 | 8.22 | 8.29 |
| 35 | 4.28 | 5.03 | 4.75 | 3.96 | 4.63 | – | – | – | – | – | – |

models. To further assess the predictive models, the correlation between measured and predicted GV values was visualized through scatter plots (Fig. 15). Also, the models' measured and predicted values on the testing dataset are listed in Table 5 to compare the accuracy of the models in practice.

Figure 15 shows the distributions of the predicted values of the hybrid models (HHOA–DNN, WOA–DNN, PSOA–DNN) on the training dataset, and it can be seen that the proposed models are better than the DNN model (without optimization). The convergence of these models was high as well, and the outliers outside the 80% confidence level are very few. Of those, the distribution of the predicted values on the HHOA–DNN model is slightly better than the remaining hybrid models. Similar results were also reported on the testing dataset of the developed models in this study. The predicted GVs on the testing dataset agree with those of the visualizations in Figure 15. The predicted results provided by the HHOA–DNN model are closer to the measured values compared with the predicted results provided by the other models.

## SENSITIVITY ANALYSIS

Herein, the HHOA–DNN model was proven to be the best model for predicting GV with high accuracy. A sensitivity analysis was performed based

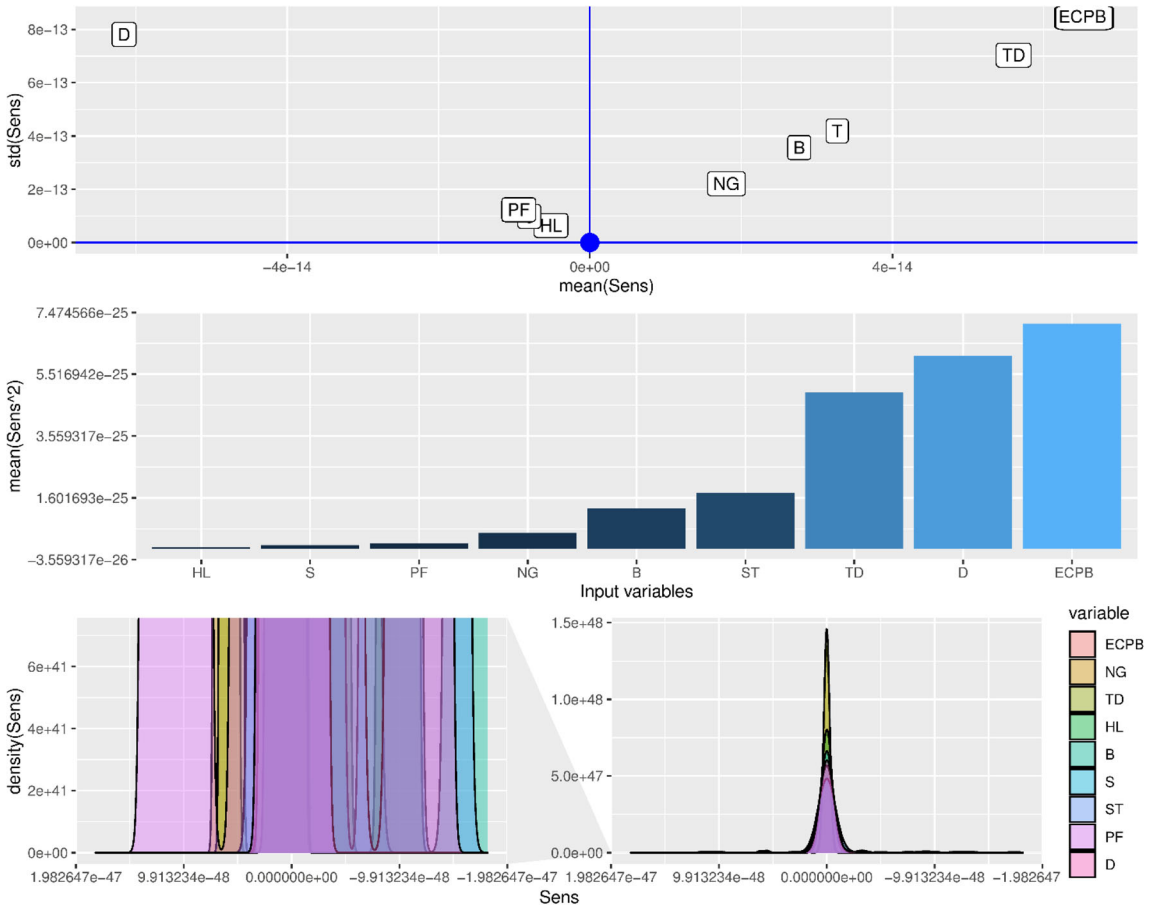


**Figure 16.** Sensitivity of the input variables for the HHOA–DNN model.

on the standard deviation, mean, and density of the input variables to investigate their influence, as shown in Figure 16. The results indicated that the ECPB, TD, and D are the most influential variables for predicting GV. In other words, these variables have a great relationship with GV, and they should be used to predict GV in mine blasting.

## CONCLUSION

In this study, optimization algorithms were used to help find optimal MLP models based on deep learning techniques, and three enhanced DNN-based models were proposed to solve the GV prediction problem in mine blasting, namely HHOA–DNN, WOA–DNN, and PSOA–DNN. The results indicated that the optimization algorithms provided better optimization results compared with the DNN model without optimization in predicting GV. Of those, the HHOA–DNN model yielded the highest accuracy compared with the other hybrid models. Compared with the WOA and PSOA optimizers, the HHOA optimizer provided the best performance, more simple design problems, and fewer parameters. Also, the sensitivity analysis results showed that the ECPB, distance, and time delay are the most important parameters for predicting GV and that they should be used as primary parameters in predicting GVs. Moreover, it was shown that the proposed HHOA–DNN is a potential solution for predicting GVs with high accuracy in practical engineering.

## ACKNOWLEDGMENTS

This paper was supported by the Ministry of Education and Training (MOET) in Viet Nam un-

der Grant Number B2020-MDA-16. The authors also thank the Center for Mining, Electro-Mechanical research of Hanoi University of Mining and Geology, Hanoi, Vietnam.

## REFERENCES


Afeni, T. B. (2009). Optimization of drilling and blasting operations in an open pit mine—The SOMAIR experience. *Mining Science and Technology (china), 19*(6), 736–739.

Amiri, M., Amnieh, H. B., Hasanipanah, M., & Khanli, L. M. (2016). A new combination of artificial neural network and K-nearest neighbors models to predict blast-induced ground vibration and air-overpressure. *Engineering with Computers, 32*(4), 631–644.

Amiri, M., Hasanipanah, M., & Bakhshandeh Amnieh, H. (2020). Predicting ground vibration induced by rock blasting using a novel hybrid of neural network and itemset mining. *Neural Computing and Applications*, *32*, 14681–14699. https://doi.org/10.1007/s00521-020-04822-w.

Armaghani, D. J., Hasanipanah, M., Amnieh, H. B., & Mohamad, E. T. (2018). Feasibility of ICA in approximating ground vibration resulting from mine blasting. *Neural Computing and Applications, 29*(9), 457–465.

Jahed Armaghani, D., Kumar, D., Samui, P., Hasanipanah, M., & Roy, B. (2020). A novel approach for forecasting of ground vibrations resulting from blasting: Modified particle swarm optimization coupled extreme learning machine. *Engineering with Computers*. https://doi.org/10.1007/s00366-020-00997-x.

Armaghani, D. J., Mahdiyar, A., Hasanipanah, M., Faradonbeh, R. S., Khandelwal, M., & Amnieh, H. B. (2016). Risk assessment and prediction of flyrock distance by combined multiple regression analysis and Monte Carlo simulation of quarry blasting. *Rock Mechanics and Rock Engineering, 49*(9), 3631–3641.

Armaghani, D. J., Momeni, E., Abad, S. V. A. N. K., & Khandelwal, M. (2015). Feasibility of ANFIS model for prediction of ground vibrations resulting from quarry blasting. *Environmental Earth Sciences, 74*(4), 2845–2860.

Arthur, C. K., Temeng, V. A., & Ziggah, Y. Y. (2020). Novel approach to predicting blast-induced ground vibration using Gaussian process regression. *Engineering with Computers, 36*(1), 29–42.

Bairathi D., & Gopalani D. (2020). A novel swarm intelligence based optimization method: Harris' hawk optimization. In: A. Abraham, A. Cherukuri, P. Melin, & N. Gandhi (Eds.), *Intelligent systems design and applications. ISDA 2018. Advances in Intelligent Systems and Computing* (Vol. 941). Springer, Cham. https://doi.org/10.1007/978-3-030-16660-1_81.

Bayat, P., Monjezi, M., Rezakhah, M., & Jahed Armaghani, D. (2020). Artificial neural network and firefly algorithm for estimation and minimization of ground vibration induced by blasting in a mine. *Natural Resources Research*, *29*, 4121–4132. https://doi.org/10.1007/s11053-020-09697-1.

Beskirli, A., & Dağ, İ. (2020). A new binary variant with transfer functions of Harris Hawks Optimization for binary wind turbine micrositing. *Energy Reports, 6*, 668–673.

Bisoyi, S., & Pal, B. (2020). Prediction of ground vibration using various regression analysis. *Journal of Mining Science, 56*(3), 378–387.

Bratton, D., & Kennedy, J. (2007). Defining a standard for particle swarm optimization. In: *2007 IEEE Swarm Intelligence Symposium* (pp. 120–127). https://doi.org/10.1109/SIS.2007.368035.

Brownlee, J. (2018). *Deep learning for time series forecasting: Predict the future with MLPs, CNNs and LSTMs in Python*. Machine Learning Mastery.

Cao, H., Qian, X., Chen, Z., & Zhu, H. (2017). Layout and size optimization of suspension bridges based on coupled modelling approach and enhanced particle swarm optimization. *Engineering Structures, 146*, 170–183.

Chen, H., Li, W., & Yang, X. (2020). A whale optimization algorithm with chaos mechanism based on quasi-opposition for global optimization problems. *Expert Systems with Applications, 158*, 113612.

Clerc, M. (2010). *Particle swarm optimization* (Vol. 93). Wiley.

Ding, X., Hasanipanah, M., Nikafshan Rad, H., & Zhou, W. (2021). Predicting the blast-induced vibration velocity using a bagged support vector regression optimized with firefly algorithm. *Engineering with Computers*, *37*, 2273–2284. https://doi.org/10.1007/s00366-020-00937-9.

Du, K. L., & Swamy, M. N. S. (2016). Particle swarm optimization. In: *Search and optimization by metaheuristics*. Birkhäuser, Cham. https://doi.org/10.1007/978-3-319-41192-7_9.

Duvall, W. I., & Petkof, B. (1959). *Spherical propagation of explosion-generated strain pulses in rock*. US Department of the Interior, Bureau of Mines. Report of Investigations 5483.

Faradonbeh, A., Majid, T., Murlidhar, M., et al. (2016). Prediction of ground vibration due to quarry blasting based on gene expression programming: A new model for peak particle velocity prediction. *International Journal of Environmental Science and Technology, 13*(6), 1453–1464.

Faramarzi, F., Farsangi, M. A. E., & Mansouri, H. (2014). Simultaneous investigation of blast induced ground vibration and airblast effects on safety level of structures and human in surface blasting. *International Journal of Mining Science and Technology, 24*(5), 663–669.

Fattahi, H., & Hasanipanah, M. (2021). Prediction of blast-induced ground vibration in a mine using relevance vector regression optimized by metaheuristic algorithms. *Natural Resources Research*, *30*, 1849–1863. https://doi.org/10.1007/s11053-020-09764-7.

Garcia-Garcia, A., Orts-Escolano, S., Oprea, S., Villena-Martinez, V., Martinez-Gonzalez, P., & Garcia-Rodriguez, J. (2018). A survey on deep learning techniques for image and video semantic segmentation. *Applied Soft Computing, 70*, 41–65.

Ghasemi, E., Sari, M., & Ataei, M. (2012). Development of an empirical model for predicting the effects of controllable blasting parameters on flyrock distance in surface mines. *International Journal of Rock Mechanics and Mining Sciences, 52*, 163–170.

Gölcük, İ., & Ozsoydan, F. B. (2021). Quantum particles-enhanced multiple Harris Hawks swarms for dynamic optimization problems. *Expert Systems with Applications*, *167*, 114202.

Goodfellow, I., Bengio, Y., Courville, A., & Bengio, Y. (2016). *Deep learning*. MIT Press Publisher. http://www.deeplearningbook.org.

Guo, H., Nguyen, H., Bui, X.-N., & Armaghani, D. J. (2019). A new technique to predict fly-rock in bench blasting based on an ensemble of support vector regression and GLMNET. *Engineering with Computers*. https://doi.org/10.1007/s00366-019-00833-x.

Hajihassani, M., Armaghani, D. J., Marto, A., & Mohamad, E. T. (2015). Ground vibration prediction in quarry blasting through an artificial neural network optimized by imperialist competitive algorithm. *Bulletin of Engineering Geology and the Environment, 74*(3), 873–886.

Han, J., Zhang, D., Cheng, G., Liu, N., & Xu, D. (2018). Advanced deep-learning techniques for salient and category-specific object detection: A survey. *IEEE Signal Processing Magazine, 35*(1), 84–100.

Hasanipanah, M., Golzar, S. B., Larki, I. A., Maryaki, M. Y., & Ghahremanians, T. (2017). Estimation of blast-induced ground vibration through a soft computing framework. *Engineering with Computers, 33*(4), 951–959.

Hasanipanah, M., Monjezi, M., Shahnazar, A., Armaghani, D. J., & Farazmand, A. (2015). Feasibility of indirect determination of blast induced ground vibration based on support vector machine. *Measurement, 75*, 289–297.

Heidari, A. A., Mirjalili, S., Faris, H., Aljarah, I., Mafarja, M., & Chen, H. (2019). Harris hawks optimization: Algorithm and applications. *Future Generation Computer Systems, 97*, 849–872.

Himanshu, V. K., Roy, M., Mishra, A., Paswan, R. K., Panda, D., & Singh, P. (2018). Multivariate statistical analysis approach for prediction of blast-induced ground vibration. *Arabian Journal of Geosciences, 11*(16), 1–11.

Huang, J., Koopialipoor, M., & Armaghani, D. J. (2020). A combination of fuzzy Delphi method and hybrid ANN-based systems to forecast ground vibration resulting from blasting. *Scientific Reports, 10*(1), 1–21.

Kahriman, A. (2002). Analysis of ground vibrations caused by bench blasting at can open-pit lignite mine in Turkey. *Environmental Geology, 41*(6), 653–661.

Kahriman, A., Ozer, U., Aksoy, M., Karadogan, A., & Tuncer, G. (2006). Environmental impacts of bench blasting at Hisarcik Boron open pit mine in Turkey. *Environmental Geology, 50*(7), 1015–1023.

Kennedy, J., & Eberhart, R. (1995). Particle swarm optimization. In: *Proceedings of ICNN'95 - International Conference on Neural Networks* (Vol. 4, pp. 1942–1948). https://doi.org/10.1109/ICNN.1995.488968.

Kiranyaz, S., Ince, T., & Gabbouj, M. (2014). *Multidimensional particle swarm optimization for machine learning and pattern recognition*. Springer.

Krithiga, R., & Ilavarasan, E. (2020). A reliable modified whale optimization algorithm based approach for feature selection to classify twitter spam profiles. *Microprocessors and Microsystems*. https://doi.org/10.1016/j.micpro.2020.103451.

Kumar, R., Choudhury, D., & Bhargava, K. (2016). Determination of blast-induced ground vibration equations for rocks using mechanical and geological properties. *Journal of Rock Mechanics and Geotechnical Engineering, 8*(3), 341–349.

Lawal, A. I., Kwon, S., & Kim, G. Y. (2021). Prediction of the blast-induced ground vibration in tunnel blasting using ANN, moth-flame optimized ANN, and gene expression programming. *Acta Geophysica, 69*, 161–174.

Lazinica, A. (2009). *Particle swarm optimization*. BoD-Books on Demand. IntechOpen.

Li, A.-D., & He, Z. (2020). Multiobjective feature selection for key quality characteristic identification in production processes using a nondominated-sorting-based whale optimization algorithm. *Computers & Industrial Engineering, 149*, 106852.

Liu, H., & Cocea, M. (2017). Semi-random partitioning of data into training and test sets in granular computing context. *Granular Computing, 2*(4), 357–386.

Mahdiyar, A., Marto, A., & Mirhosseinei, S. A. (2018). Probabilistic air-overpressure simulation resulting from blasting operations. *Environmental Earth Sciences, 77*(4), 123.

Maleki, A., Haghighi, A., Irandoost Shahrestani, M., & Abdelmalek, Z. (2021). Applying different types of artificial neural network for modeling thermal conductivity of nanofluids containing silica particles. *Journal of Thermal Analysis and Calorimetry*, *144*, 1613–1622. https://doi.org/10.1007/s10973-020-09541-x.

Mirjalili, S., & Lewis, A. (2016). The whale optimization algorithm. *Advances in Engineering Software, 95*, 51–67.

Moayedi, H., Osouli, A., Nguyen, H., & Rashid, A. S. A. (2021). A novel Harris hawks' optimization and k-fold cross-validation predicting slope stability. *Engineering with Computers*, *37*, 369–379. https://doi.org/10.1007/s00366-019-00828-8.

Mohammadi, D., Mikaeil, R., & Abdollahi-Sharif, J. (2020). Implementation of an optimized binary classification by GMDH-type neural network algorithm for predicting the blast produced ground vibration. *Expert Systems, 37*(5), e12563.

Molaei, S., Moazen, H., Najjar-Ghabel, S., & Farzinvash, L. (2021). Particle swarm optimization with an enhanced learning strategy and crossover operator. *Knowledge-Based Systems*. https://doi.org/10.1016/j.knosys.2021.106768.

Monjezi, M., Bahrami, A., Varjani, A. Y., & Sayadi, A. R. (2011). Prediction and controlling of flyrock in blasting operation using artificial neural network. *Arabian Journal of Geosciences, 4*(3–4), 421–425.

Munagala, V. K., & Jatoth, R. K. (2021). Design of fractional-order PID/PID controller for speed control of DC motor using harris hawks optimization. In: R. Kumar, V. P. Singh, A. Mathur (Eds.) *Intelligent algorithms for analysis and control of dynamical systems*. Algorithms for Intelligent Systems. Springer, Singapore. https://doi.org/10.1007/978-981-15-8045-1_11.

Murlidhar, B. R., Armaghani, D. J., & Mohamad, E. T. (2020). Intelligence prediction of some selected environmental issues of blasting: A review. *The Open Construction & Building Technology Journal*, *14*, 298–308. https://doi.org/10.2174/1874836802014010298.

Nateghi, R. (2011). Prediction of ground vibration level induced by blasting at different rock units. *International Journal of Rock Mechanics and Mining Sciences, 48*(6), 899–908.

Nguyen, H., Bui, X.-N., Bui, H.-B., & Mai, N.-L. (2018). A comparative study of artificial neural networks in predicting blast-induced air-blast overpressure at Deo Nai open-pit coal mine, Vietnam. *Neural Computing and Applications, 32*(8), 3939–3955.

Nguyen, H., Bui, X.-N., Choi, Y., Lee, C. W., & Armaghani, D. J. (2020). A Novel combination of whale optimization algorithm and support vector machine with different kernel functions for prediction of blasting-induced fly-rock in quarry mines. *Natural Resources Research*. https://doi.org/10.1007/s11053-020-09710-7.

Nguyen, H., Bui, X.-N., & Moayedi, H. (2019a). A comparison of advanced computational models and experimental techniques in predicting blast-induced ground vibration in open-pit coal mine. *Acta Geophysica, 67*(4), 1025–1037.

Nguyen, H., Bui, X.-N., Tran, Q.-H., & Mai, N.-L. (2019b). A new soft computing model for estimating and controlling blast-produced ground vibration based on hierarchical K-means clustering and cubist algorithms. *Applied Soft Computing, 77*, 376–386. https://doi.org/10.1016/j.asoc.2019.01.042.

Ozer, U., Kahriman, A., Aksoy, M., Adiguzel, D., & Karadogan, A. (2008). The analysis of ground vibrations induced by bench blasting at Akyol quarry and practical blasting charts. *Environmental Geology, 54*(4), 737–743.

Poli, R., Kennedy, J., & Blackwell, T. (2007). Particle swarm optimization. *Swarm Intelligence, 1*(1), 33–57.

Qi, W. (2021). Optimization of cloud computing task execution time and user QoS utility by improved particle swarm optimization. *Microprocessors and Microsystems, 80*, 103529.

Qian, X., Jia, S., Huang, K., Chen, H., Yuan, Y., & Zhang, L. (2020). Optimal design of Kaibel dividing wall columns based on improved particle swarm optimization methods. *Journal of Cleaner Production, 273*, 123041. https://doi.org/10.1016/j.jclepro.2020.123041.

Radha, R., & Gopalakrishnan, R. (2020). A medical analytical system using intelligent fuzzy level set brain image segmentation based on improved quantum particle swarm optimization. *Microprocessors and Microsystems, 79*, 103283.

Salman, A. G., Kanigoro, B., & Heryadi, Y. (2015). Weather forecasting using deep learning techniques. In: *2015 international conference on advanced computer science and information systems (ICACSIS)* (pp. 281–285). https://doi.org/10.1109/ICACSIS.2015.7415154.

Senthil Kumar, A., Sudheer, K., Jain, S., & Agarwal, P. (2005). Rainfall-runoff modelling using artificial neural networks: Comparison of network types. *Hydrological Processes: An International Journal, 19*(6), 1277–1291.

Setiawan, I., Yusnitasari, T., Nurhady, H., & Hizviani, N. V. (2020). Implementation of convolutional neural network method for classification of Baum Test. In: *2020 fifth international conference on informatics and computing (ICIC)* (pp. 1–6). https://doi.org/10.1109/ICIC50835.2020.9288595.

Shankar, N., & SaravanaKumar, N. (2020). Reduced partial shading effect in multiple PV array configuration model using MPPT based enhanced particle swarm optimization technique. *Microprocessors and Microsystems*. https://doi.org/10.1016/j.micpro.2020.103287.

Singh, A., & Khamparia, A. (2020). A hybrid whale optimization-differential evolution and genetic algorithm based approach to solve unit commitment scheduling problem: WODEGA. *Sustainable Computing: Informatics and Systems, 28*, 100442.

Singh, C. P., Agrawal, H., & Mishra, A. K. (2020). A study on influence of blast-induced ground vibration in dragline bench blasting using signature hole analysis. *Arabian Journal of Geosciences, 13*(13), 1–9.

Sulaiman, N., Taib, M. N., Lias, S., Murat, Z. H., Aris, S. A. M., & Hamid, N. H. A. (2011). EEG-based stress features using spectral centroids technique and k-nearest neighbor classifier. In: *2011 UkSim 13th international conference on computer modelling and simulation* (pp. 69–74). https://doi.org/10.1109/UKSIM.2011.23.

Wang, H., Peng, M.-J., Ayodeji, A., Xia, H., Wang, X.-K., & Li, Z.-K. (2021). Advanced fault diagnosis method for nuclear power plant based on convolutional gated recurrent network and enhanced particle swarm optimization. *Annals of Nuclear Energy, 151*, 107934.

Yan, Z., Zhang, J., Zeng, J., & Tang, J. (2021). Nature-inspired approach: An enhanced whale optimization algorithm for global optimization. *Mathematics and Computers in Simulation, 185*, 17–46.

Yang, H., Hasanipanah, M., Tahir, M. M., & Tien Bui, D. (2020). Intelligent prediction of blasting-induced ground vibration using ANFIS optimized by GA and PSO. *Natural Resources Research*, *29*, 739–750. https://doi.org/10.1007/s11053-019-09515-3.

Yang, H., Rad, H. N., Hasanipanah, M., Amnieh, H. B., & Nekouie, A. (2020). Prediction of vibration velocity generated in mine blasting using support vector regression improved by optimization algorithms. *Natural Resources Research, 29*(2), 807–830.

Yegnanarayana, B. (2006). *Artificial neural networks*. PHI Learning Pvt. Ltd. New Delhi.

Yu, C., Koopialipoor, M., Murlidhar, B. R. Mohammed, A. S., Armaghani, D. J., Mohamad, E. T., & Wang, Z. (2021). Optimal ELM–harris hawks optimization and ELM–grasshopper optimization models to forecast peak particle velocity resulting from mine blasting. *Natural Resources Research*, *30*, 2647–2662. https://doi.org/10.1007/s11053-021-09826-4.

Yu, Z., Shi, X., Zhou, J., Gou, Y., Huo, X., Zhang, J., & Armaghani, D. J. (2020). A new multikernel relevance vector machine based on the HPSOGWO algorithm for predicting and controlling blast-induced ground vibration. *Engineering with Computers*. https://doi.org/10.1007/s00366-020-01136-2.

Zeng, N., Song, D., Li, H., You, Y., Liu, Y., & Alsaadi, F. E. (2021). A competitive mechanism integrated multi-objective whale optimization algorithm with differential evolution. *Neurocomputing, 432*, 170–182.

Zhang, S., Bui, X.-N., Trung, N.-T., Nguyen, H., & Bui, H.-B. (2020a). Prediction of rock size distribution in mine bench blasting using a novel ant colony optimization-based boosted regression tree technique. *Natural Resources Research, 29*(2), 867–886.

Zhang, Y., Zhou, X., & Shih, P.-C. (2020b). Modified Harris Hawks Optimization algorithm for global optimization problems. *Arabian Journal for Science and Engineering, 45*(12), 10949–10974.

Zhou, J., Asteris, P. G., Armaghani, D. J., & Pham, B. T. (2020). Prediction of ground vibration induced by blasting operations through the use of the Bayesian Network and random forest models. *Soil Dynamics and Earthquake Engineering, 139*, 106390.

Zou J., Han Y., & So, S. S. (2008). Overview of artificial neural networks. In: D. J. Livingstone (Ed.) *Artificial neural networks. Methods in Molecular Biology*™ (Vol. 458). Humana Press. https://doi.org/10.1007/978-1-60327-101-1_2.